THE CELESTIAL FRAME AT FOUR RADIO FREQUENCIES

C. S. JACOBS
Jet Propulsion Laboratory, California Institute of Technology/NASA
4800 Oak Grove Dr., Pasadena CA 91109
e-mail: Chris.Jacobs@jpl.nasa.gov

ABSTRACT: The International Celestial Reference Frame (ICRF) adopted by the IAU in 1997 was based on VLBI measurements at S/X-band radio frequencies of 2.3/8.4 GHz and complemented by HIPPARCOS measurements at optical frequencies. At that time, the IAU encouraged the astrometric community to extend the ICRF to other frequencies. In response, VLBI measurements have been made at 24, 32, and 43 GHz. We discuss the programmatic and scientific motivations for extending the ICRF to these higher frequencies. This paper reviews results to date including evidence that these new high frequency frames are rapidly approaching the accuracy of the S/X-band ICRF. Prospects for future improvements of high frequency radio reference frames are also discussed.

1. INTRODUCTION

For about three decades now, radio frequency work in global astrometry, geodesy, and deep space navigation has been done at S/X-band (2.3/8.4 GHz) and has been tremendously successful in producing 100 μas level global astrometry (e.g. Ma et al, 1998; Fey et al, 2004; Petrov, 2008) and sub-cm geodesy. In response to the IAU's call to extend the ICRF to new frequencies (IAU, 1997), development work over the last decade has enabled astrometric observing at 24, 32, and 43 GHz. This paper is a review of global astrometric frames at 24, 32, and 43 GHz with comparison to the traditional 2.3/ 8.4 GHz frames.

Why these new frequencies? Increasing observing frequencies by factor of 3 to 5 has several advantages. For tracking of spacecraft in deep space, the driver is the potential for higher telemetry data rates to and from probes. Other advantages include 1) the spatial distribution of flux becomes significantly more compact lending hope that the positions will be more stable over time (Charlot et al, 2008), 2) Radio Frequency Interference (RFI) at S-band would be avoided, 3) Ionosphere and solar plasma effects on group delay are reduced by a factor of 9 to 25!

While these are very significant advantages, there are also disadvantages. Observing above 8.4 GHz moves one closer to the water vapor line at 22 GHz and thus increases the system temperature from a few Kelvins per atmospheric thickness up to 10–15 Kelvins per atmosphere or more. Thus one becomes much more sensitive to weather. Furthermore, the sources themselves are in general weaker and many sources are resolved. Also, with the observing wavelengths shortened by a factor of 3 to 5, the coherence times are shortened so that practical integration times are a few minutes or less—even in relatively dry climates. The shorter wavelengths also imply that the antenna pointing accuracy requirements must be tightened by the same factor of 3 to 5. The combined effect of these disadvantages is to lower the system sensitivity. Fortunately, recent advances in recording technology make it feasible and affordable to offset these losses in sensitivity by recording more bits.

This paper is organized as follows: We will describe the observations & modelling, and review the resulting frames. Next, we will estimate the accuracy by comparing the X/Ka frame to a recent S/X frame. This will be complemented by a discussion of the error budget. Finally, we will provide conclusions and anticipated directions for further research.

2. OBSERVATIONS & RESULTS

At the time of this report, celestial reference frames have been produced at four radio frequencies: S/X-band (2.3/ 8.4 GHz), K-band (24 GHz), Q-band (43 GHz), and X/Ka-band (8.4/ 32 GHz). All these frames cover the full 24 hours of right ascension. Only the S/X frames cover the full range of declinations. The original S/X-band ICRF (Ma et al, 1998) was produced in 1995 based on 1.6M observations resulting in 608 source positions (Fig. 1). More recent S/X frames benefit from much larger data sets. For example,

the 2008b-astro frame (Petrov, 2008) uses about 5M observations from a variety of networks around the globe to produce a frame of $\approx$ 3500 sources of which $\approx$ 2400 have position uncertainties of less than 1 mas (Fig 2). At K-band 82K observations (Lanyi et al, 2008) are used to produce a frame of 275 sources covering down to about -40° declination (Fig. 3). At Q-band 19K observations (Lanyi et al, 2008) produce a frame of 132 sources covering down to roughly -30°. (Fig 4). At X/Ka-band 7K observations (Jacobs & Sovers, 2008) produce a frame of 321 sources covering down to -45° (Fig. 5). As can be seen from Figs. 1–5, all current radio frames are significantly weaker in the southern hemisphere. This is due to the scarcity of southern stations. In particular, the K and Q-band frames are based on the all-northern VLBA and the X/Ka frame uses only one southern station. Even the S/X frame with its full sky coverage has a very limited number of observations in the far south. In Figs. 1–5, the sources are coded according to their 1-σ formal declination uncertainties with the value ranges indicated in the figure's legend. Note that on average, the declination precision decreases as one moves toward the south for all frames.

While there are some modelling variations amongst the various catalogs, the description of Sovers *et al* (1998) is a fair first approximation. For further details the reader is referred to the papers cited for each frame described above.

3. ACCURACY

Experience shows that formal uncertainties tend to underestimate true errors. External estimates of errors were obtained by comparing X/Ka-band RA and declinations to estimates from analysis of S/X data. For the 273 sources in common, the weighted RMS (wRMS) differences are 235 μas in RA cos(dec) and 285 μas in declination. These differences reveal decreasing accuracy RA and declination as one moves south. For K and Q-band accuracy see Lanyi et al (2008).

In astrometry, it is usually much easier to measure the relative positions of nearby sources than to accurately measure sources that are separated by long arcs. In order to investigate this tendency, we calculated for both X/Ka and S/X the arclengths between all pairs of sources, binned them in 5 deg bins and then differenced the arcs. We then took the mean arclength difference for each bin. As expected, arclengths agree better for short arcs and gradually worsen as arcs grow longer out to a mean difference of 70 μas at arcs of 90 deg. This is one measure of the level of zonal errors in our comparison.

4. ERROR BUDGET

Having assessed the size of errors in X/Ka positions using the much larger S/X data set as a standard of accuracy, we now discuss the major contributions to the errors of the X/Ka measurements: SNR, instrumentation, and troposphere. Figure 6 shows the weighted RMS group delay vs. log10 of the Ka-band SNR. We conclude that for SNR < 30, the thermal error dominates the error budget. For higher SNRs, troposphere and instrumentation errors become important. Binning of wRMS delay vs. airmass thickness shows that troposphere is not the dominant error due to the generally low SNRs just mentioned. However, the phase rates (which carry much less weight in the fit) are dominated by errors from tropospheric mismodelling, thus hinting that troposphere will become more important as our SNR improves (Treuhaft & Lanyi, 1987; Bar-Sever et al 2007). The last major category of errors comes from un-calibrated instrumentation. A proto-type phase calibrator has been developed for calibrating from the feed to the digitizer (Hamell et al, 2003). Test data indicate an approximately diurnal instrumental effect with $\approx$180 psec RMS. Although the data themselves can be used to partially parameterize this effect, we believe that phase calibrators will be needed in order to achieve accuracy of better than 200 μas in a timely manner.

5. CONCLUSIONS

The challenge has been met to extend the S/X-based ICRF to 3 to 5 times higher frequencies with frames now being produced at 24, 32, and 43 GHz. For now, S/X frames still have better global coverage and better formal uncertainties and in all likelihood better true accuracy. However, the frames at 24, 32, and 43 GHz now have accuracies on the order of 1/4 mas. At K-band, incomplete calibration of plasma and tropospheric effects limits accuracy. Compared to K-band, at Q-band plasma errors are 4 times less, but weaker sources and shorter atmospheric coherence times lead to SNR limited accuracy. Like Q-band, X/Ka-band has SNR issues and has worse instrumental errors due to the lack of instrumental

phase calibrations. We expect the instrinsic source structure at frequencies above 8 GHz to become more compact thereby enticing observers with the potential for frames which are more stable and perhaps eventually more accurate than the S/X-based ICRF.

Acknowledgements. The research described in this paper was performed at the Jet Propulsion Laboratory of the California Institute of Technology, under a contract with the National Aeronautics and Space Administration. Copyright © 2009 by California Institute of Technology. Government sponsorship acknowledged. X/Ka data were collected with NASA's Deep Space Network. K and Q-band data were acquired an analyzed by the KQ VLBI Collaboration using data from the NSF's VLBA instrument (see Lanyi et al [2008] for a full list of collaborators). We thank the staff from both the DSN and the VLBA.

6. REFERENCES

Bar-Sever, Y. E., et al, 2007, 'Atmospheric Media Calibration for the Deep Space Network,' Proceedings of the IEEE (Special issue), 95, 11.

Charlot, P., et al, 2008, 'The Celestial Reference Frame at Higher Radio Frequencies II. VLBA Imaging at 24 and 43 GHz,' submitted to AJ .

Fey, A. L., et al, 2004, 'The Second Extension of the ICRF: ICRF-Ext.2', AJ , 127, pp. 3587-3608.

Hamell, R., Tucker, B., & Calhoun, M., 2003 'Phase Calibration Generator,' JPL IPN Prog. Report 42-154, pp. 1-14.

IAU General Assembly XXIII, Resolution B2-d, Kyoto, Japan, August 1997.
iau.org/static/resolutions/IAU1997_French.pdf

Jacobs, C.S., & Sovers, O. J., 2008, 'Extending the ICRF to Higher Radio Frequencies: Global Astrometric Results at 32/8 GHz,' IVS 2008 General Meeting Proc., St. Petersburg, Russia., D. Behrend and K. D. Baver, eds.

Lanyi, G. E. et al, 2008, 'Extraglactic Celestial Reference Frames at 24 and 43 GHz: Global Astrometric Results from the VLBA', submitted to AJ .

Ma, C., et al, 1998, 'The International Celestial Reference Frame as Realized by Very Long Baseline Interferometry', AJ , 116, 1, pp. 516-546.

Petrov, L., 'VLBI global solution 2008b_astro,' *modified to use uninflated errors as provided by D. Gordon of NASA Goddard Space Flight Center.*
http://vlbi.gsfc.nasa.gov/astro/

Sovers, O. J., J. L. Fanselow, C. S. Jacobs, 1998, 'Astrometry and Geodesy with Radio Interferometry: Experiments, Models, Results,' Rev. Mod. Phys., 70, 4.

Treuhaft, R. N. & Lanyi, G.E., 1987, 'The Effect of the Dynamic Wet Troposphere on Radio Interferometric Measurements,' Radio Science, 22, pp. 251-65.

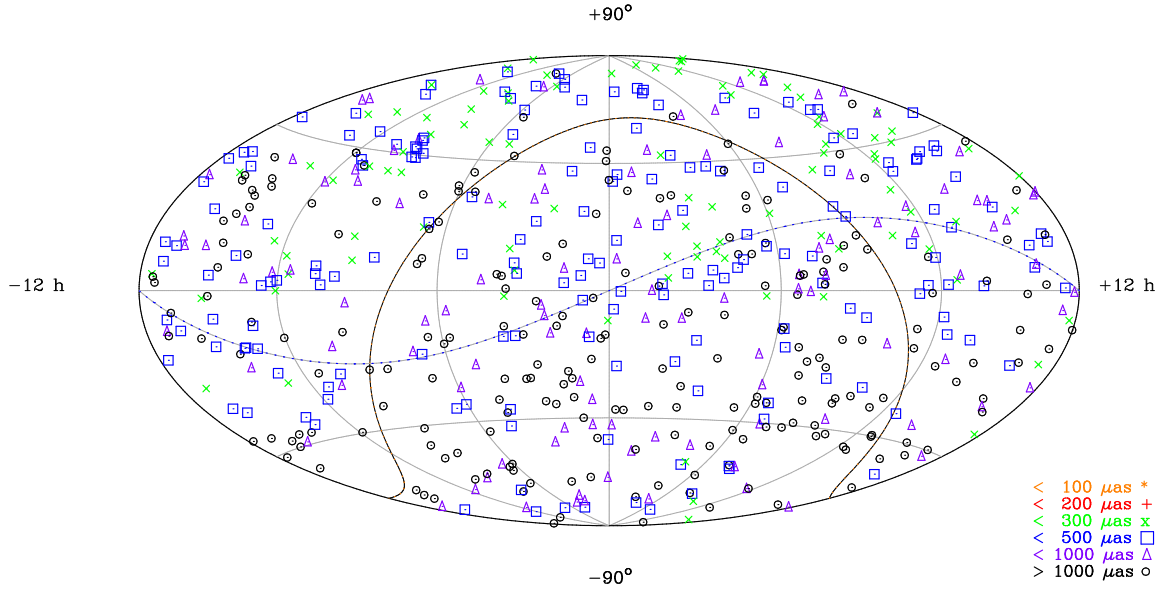

Figure 1: 608 S/X-band sources of the original ICRF based on a 1995 solution (Ma et al, 1998). Symbols indicate 1-σ formal declination uncertainties with size bins defined in the legend at lower right. (α, δ) = $(0, 0)$ is at the center. The ecliptic plane is indicated by a dashed line. The galactic plane is indicated as a black line approximately shaped like an Ω.

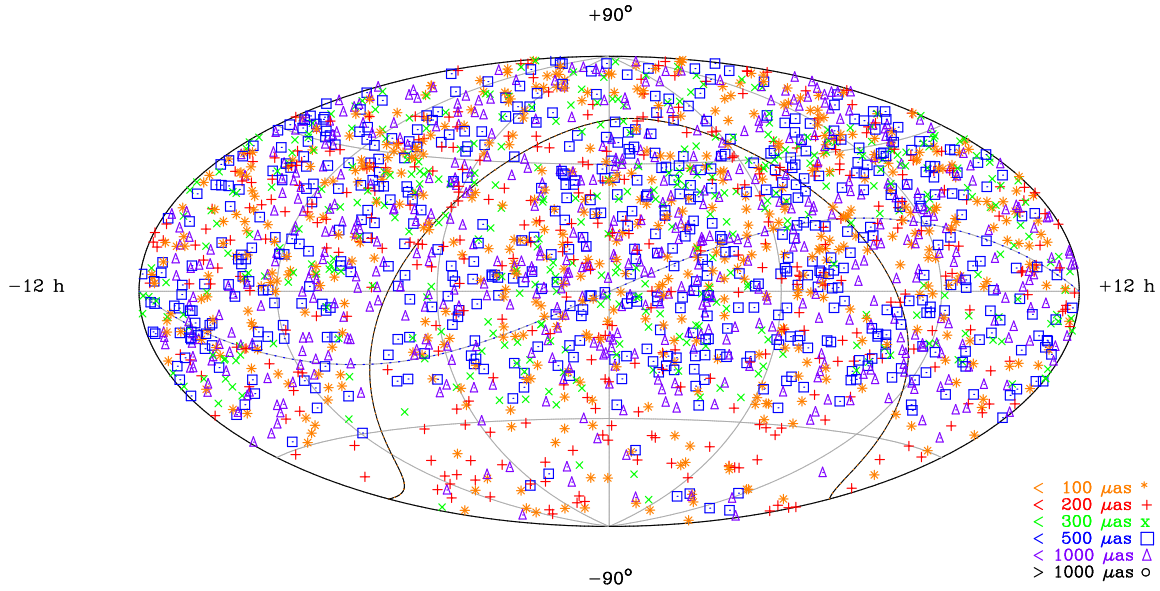

Figure 2: $\approx$ 2400 S/X sources from the 2008b-astro catalog with uncertainties < 1 mas (Petrov, 2008) . Symbols indicate 1-σ formal declination uncertainties with size bins defined in the legend at lower right. (α, δ) = $(0, 0)$ is at the center. The ecliptic plane is indicated by a dashed line. The galactic plane is indicated as a black line approximately shaped like an Ω.

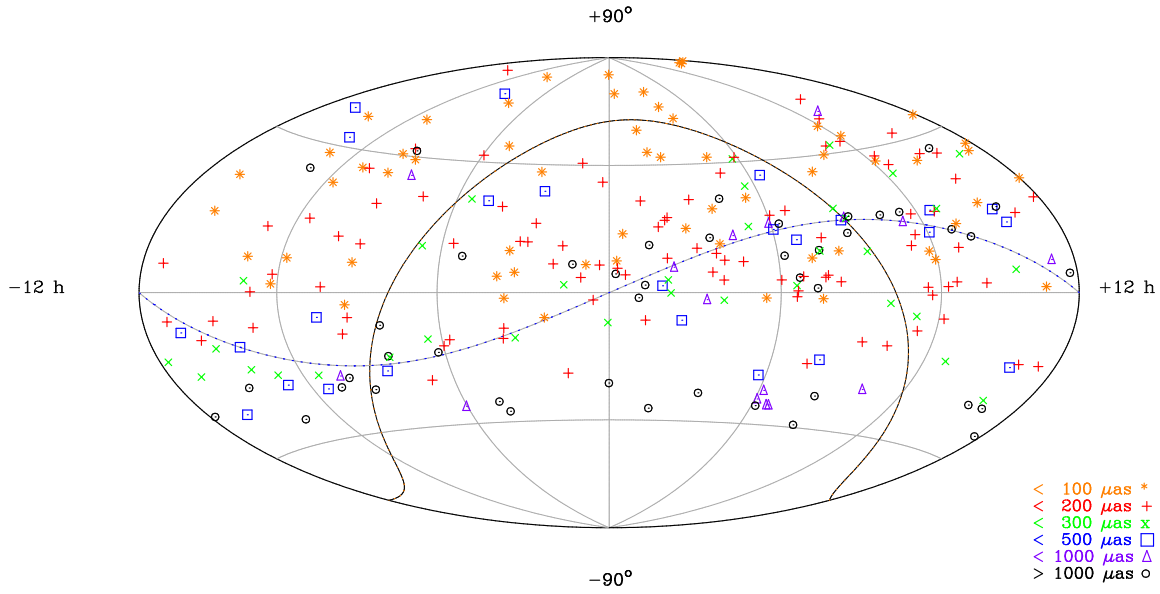

Figure 3: Distribution of 275 K-band sources detected to date (Lanyi et al, 2008). Symbols indicate 1-σ formal declination uncertainties with size bins defined in the legend at lower right. $(\alpha, \delta) = (0, 0)$ is at the center. The ecliptic plane is indicated by a dashed line. The galactic plane is indicated as a black line approximately shaped like an Ω.

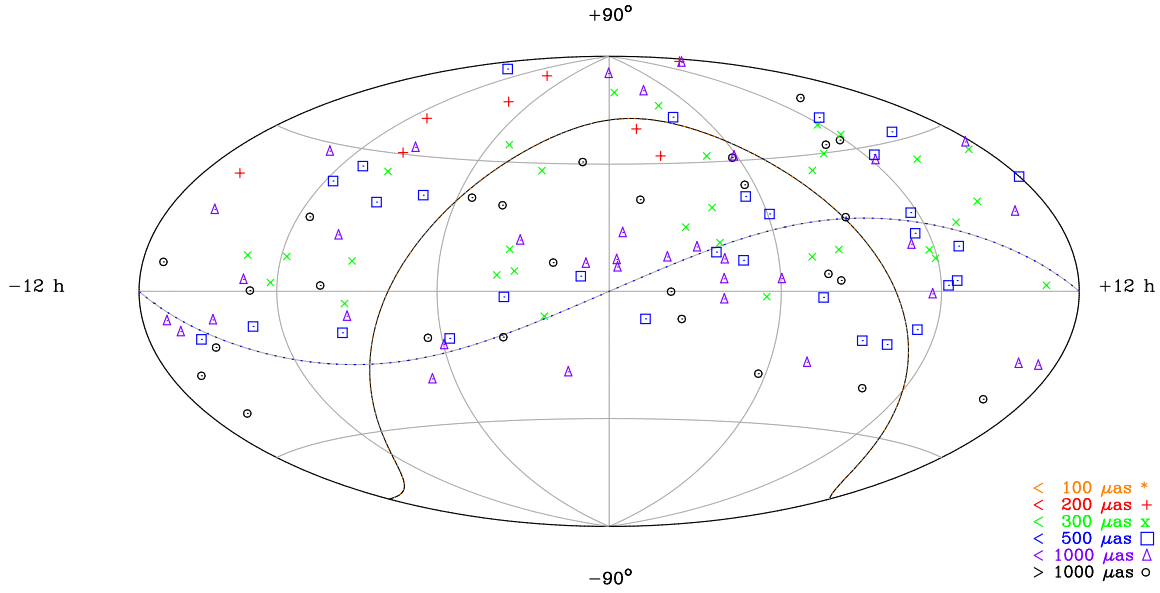

Figure 4: Distribution of 132 Q-band sources detected to date (Lanyi et al, 2008). Symbols indicate 1-σ formal declination uncertainties with size bins defined in the legend at lower right. $(\alpha, \delta) = (0, 0)$ is at the center. The ecliptic plane is indicated by a dashed line. The galactic plane is indicated as a black line approximately shaped like an Ω.

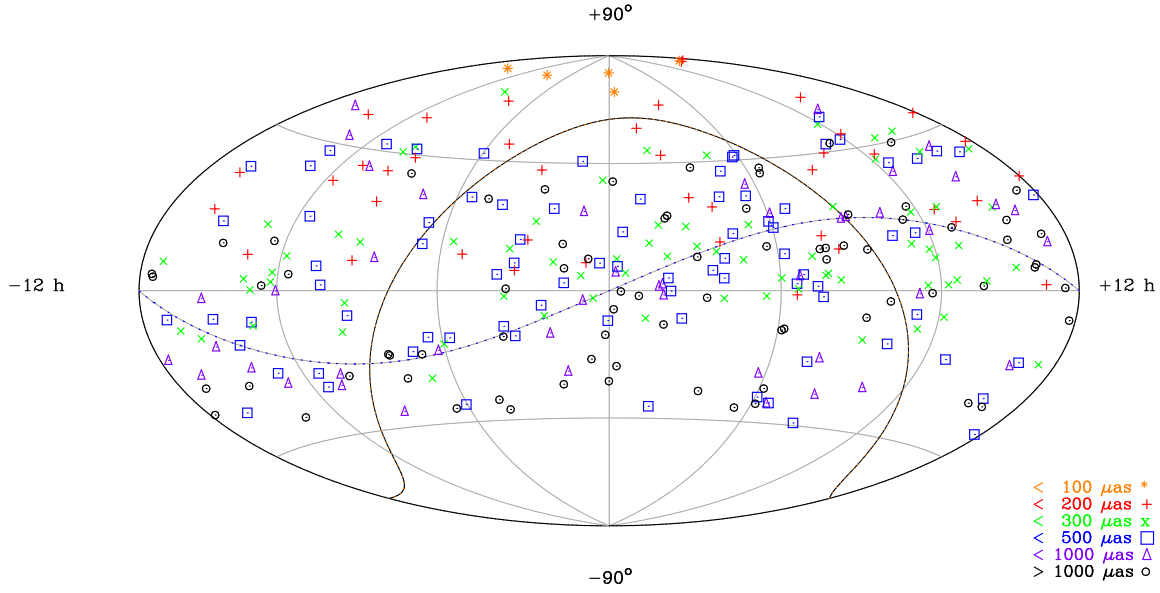

Figure 5: Distribution of 321 X/Ka-band sources detected to date (Jacobs & Sovers, 2008). Symbols indicate 1-σ formal declination uncertainties with size bins defined in the legend at lower right. $(\alpha, \delta) = (0, 0)$ is at the center. The ecliptic plane is indicated by a dashed line. The galactic plane is indicated as a black line approximately shaped like an Ω.

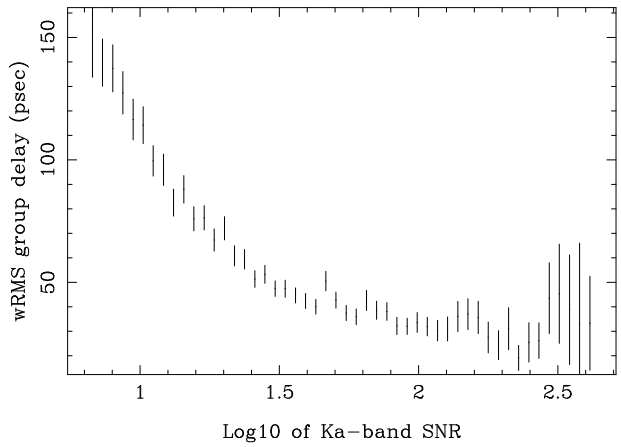

Figure 6: The wRMS residual group delay vs. the log10 of the Ka-band SNR. Note the noise floor of ≈30 psec as other error sources such as troposphere and instrumentation begin to dominate once the SNR becomes > 30.